TUTORIAL REVIEW

Check for updates

Mechanism of lithium ion selectivity through membranes: a brief review

Jian Zhang, Qiang Gao, [iD] Bo Han [iD]* and Chenggang Zhou [iD]

The recycling and reuse of lithium resources from spent lithium-ion batteries have become a major research area to address the contradiction between limited resources and increasing market demand. Membrane separation, as a highly efficient and easy-to-operate process, has attracted more attention among various lithium recycling technologies. However, the complicated ion migration process results in an insufficient understanding of the lithium ion diffusion mechanism in membrane separation. In this review, recent research efforts on membrane separation technology for lithium recovery are summarized, with the mechanism of ion selectivity through membranes being emphasized. To illustrate the ion diffusion mechanism, the ion transportation process through a membrane is divided into 3 sequential stages: the entering of ions into the channel openings of the membrane, the diffusion of ions within the channels, and the returning of ions to the solution on the other side of the membrane. In each stage, the main factors that affect lithium ion selectivity through membranes are discussed, including the ion charge, hydration energy, channel size and functional groups. It is found that the selectivity of the membrane separation process is highly correlated to the ion hydration energy and the interaction between the ion and the functional groups. In particular, the ion hydration energy is the key factor affecting the entry stage, while the anchoring strength between the ion and the functional groups of the channel wall dominates the diffusion stage within the channel. We conclude with a discussion of the challenges and future development trends of membrane separation technology for lithium recovery.

Water impact

The continuous expansion of the lithium-ion battery market gives rise to a rapid increase in lithium prices. In this review, we focus on recent research efforts on membrane separation technology for lithium recovery to further elucidate the mechanism of ion selectivity through membranes. This review would help researchers to understand the mechanism of ion selectivity through membranes and achieve lithium ion separation efficiently.

1. Introduction

Lithium-ion batteries are widely used in our daily life due to their high energy density, wide voltage range, long cycle period, light weight and other advantages.[1,2] Consequently, it is expected that the global lithium-ion battery market size will steadily increase from $40.5 billion in 2020 to $116.6 billion by 2030.[3] However, the continuous expansion of the lithium-ion battery market gives rise to a rapid increase in lithium prices. By June 2023, the price of Li_2CO_3 per ton has increased to 43 000 USD. Lithium exists mostly in the form of compounds in nature, mainly distributed in minerals, salt lake brine, seawater, *etc.*[4,5] To reconcile the contradiction between the limited lithium resources in nature and the

increasing market demand, people are now turning their attention to searching for new lithium sources.

Recycling and reusing lithium from waste lithium-ion batteries is widely recognized as the most feasible and promising solution to cope with the shortage of lithium. It is believed that the number of waste lithium-ion batteries that can be recycled worldwide will reach 641 595 tons by 2025. Especially in China, this value will reach 417 165 tons.[6] Extracting lithium resources from waste lithium-ion batteries can not only meet the huge demand for lithium in the market but also achieve waste utilization, which is a very economical green chemical process. Therefore a lot of efforts have been made to develop more efficient separation and enrichment technologies, such as chemical precipitation,[7,8] solvent extraction,[9,10] and membrane separation.[11,12]

In particular, the chemical precipitation method is mainly based on the solubility difference between various metal

Faculty of Materials Sciences and Chemistry, China University of Geosciences Wuhan, Wuhan 430074, China. E-mail: hanbo@cug.edu.cn

This journal is © The Royal Society of Chemistry 2024

Environ. Sci.: Water Res. Technol., 2024, **10**, 1305–1318 | **1305**

salts, where a large amount of precipitant is usually required.[13] The solvent extraction method takes advantage of the difference in the partition coefficients of lithium ions in two immiscible solvents for separation. However, the extraction process is time-consuming, environmentally unfriendly and requires a lot of organic solvents.[14]

Compared to other separation and enrichment methods, the membrane separation method has the advantages of convenience, high separation purity and low energy consumption.[15,16] Therefore, the membrane separation method has a wide range of applications, which can be used not only to extract lithium from waste lithium-ion batteries but also for the separation of other substances and seawater desalination.[17,18] Generally, the reported membranes include thin film composite (TFC) membranes,[19,20] covalent organic framework (COF) membranes,[21,22] metal–organic framework (MOF) membranes[23] and so on. The TFC membrane features an ultrathin selective layer above a support in cross-sectional structure with different chemical compositions, while the MOF and COF membranes usually present a large number of pores. To simplify the description, both the selective layer and the pores are referred to as channels hereafter.

Currently, membrane separation processes mainly include forward osmosis (FO),[24,25] nanofiltration (NF),[26,27] reverse osmosis (RO),[28,29] electrodialysis (ED)[30,31] and membrane capacitive deionization (MCDI).[32,33] FO technology is not very selective in solutions containing high concentrations of lithium, and RO technology is known for its high energy consumption. The ED and MCDI processes mainly rely on selective anion exchange membranes (AEMs) and cation exchange membranes (CEMs). Although ED and MCDI exhibit very rapid separation rates, the performance of ion exchange membranes can be influenced by several factors, such as membrane price and operating temperature. In contrast, NF is the most promising approach for lithium separation due to its low cost, process sustainability and low footprint.[34,35]

For a typical membrane separation process, the different rates at which different ions pass through the membrane contribute to the ion selectivity of the membrane.[36] The current explanation for membrane separation mainly includes the ion dehydration mechanism[37] and ion–channel wall interaction mechanism.[38,39] Many factors, such as channel size, hydration energy and the interaction between ions and channel walls, may affect ion selectivity through membranes.[40] In fact, ion migration across a membrane is a very complicated process, which could be influenced simultaneously by the factors mentioned above. However, there are few papers summarizing these influencing issues today, especially in the lithium recycling process. Therefore, this review will focus on recent research efforts on membrane separation technology for lithium recovery to further elucidate the mechanism of ion selectivity through membranes. Firstly, the three main stages of ion selectivity through membranes will be summarized, followed by the main factors affecting ion selectivity through membranes in

each stage. Finally, the existing main problems and possible solutions in this field will be highlighted.

2. Mechanism of ion selectivity through membranes

The entire process of ions passing through a membrane can be divided into three successive stages: (i) the first stage is the entering process of ions into the membrane, during which partial dehydration occurs; (ii) the second stage is the ion diffusion inside the membrane, during which ions may interact with functional groups on the membrane; (iii) the third stage is the returning of ions from the membrane to the solution on the other side, during which rehydration of ions may occur[41,42] (Fig. 1). In particular, the ion selectivity resulting from the first stage is called partition selectivity, while the ion selectivity generated in the second stage is called diffusion selectivity.[42] For the third stage, due to its symmetrical relationship with the first stage in the free energy curve, it can be considered that the third stage is the inverse process of the first stage.[40] In practical research, the third stage is rarely utilized to achieve ion selective passage through channels. Therefore, the following discussion will focus only on the first and second stages.

2.1. The entering process of ions into the membrane

The entering process refers to the entry of ions from the solution environment into the channel opening of the membrane under a certain driving force. Generally, the driving forces for ions passing through the membrane are mainly divided into osmotic pressure driving ($\Delta\pi$), hydraulic driving (ΔP) and electric potential driving (ΔV).[36]

Among them, osmotic pressure driving corresponds to FO technology.[43,44] As shown in Fig. 2(a), the device consists of a solution with lower concentration on the left side (feed solution), a membrane and a solution with higher concentration on the right side (draw solution). The membrane is composed of a support layer and a selective layer. Here, the role of the support layer is to maintain the mechanical stability of the membrane, while the role of the selective layer is to hinder the migration of solutes to the solution on the other side. The different concentrations between the two sides of the membrane will lead to osmotic pressure, which drives water molecules to migrate from the left solution through the membrane to the right solution. Meanwhile, the solute ions are blocked by the selective layer on the membrane. As the permeation time increases, the volume of the left solution decreases and the solute is enriched.

Hydraulic driving corresponds to NF technology[45] and RO technology.[46,47] The difference between these two technologies mainly lies in the size of the particles being filtered. NF is used to filter particles of 8 to 50 Å size from its fluid.[48] In contrast, RO is increasingly applied for water desalination and can separate contaminations of size 12 Å and less.[48] As shown in

1306 | *Environ. Sci.: Water Res. Technol.*, 2024, **10**, 1305–1318

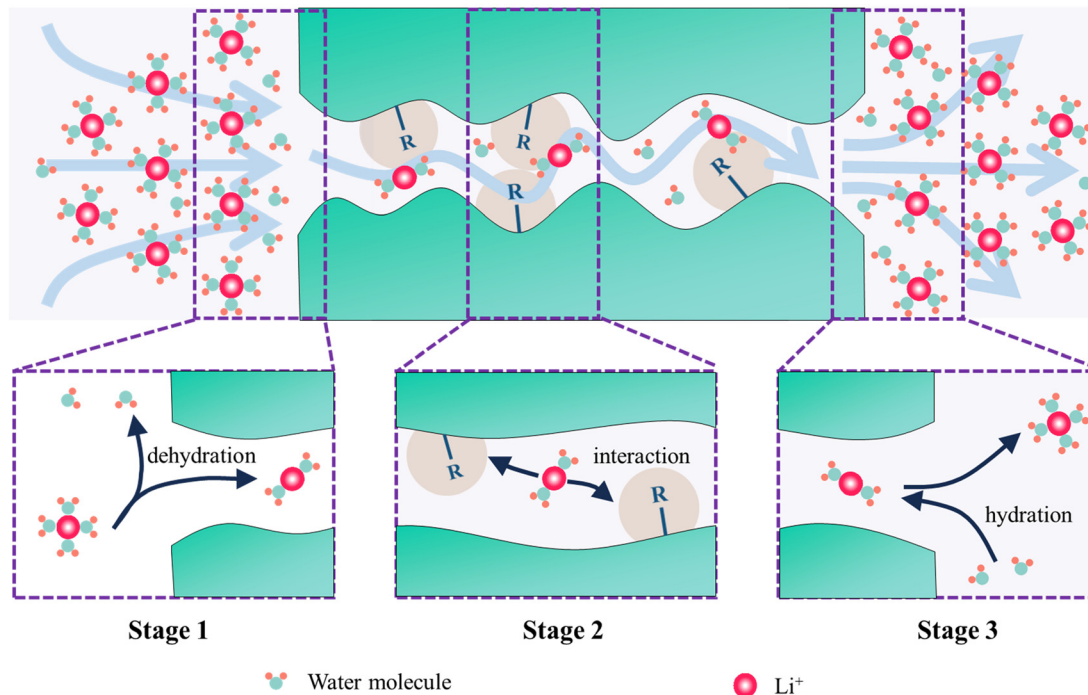This journal is © The Royal Society of Chemistry 2024

Fig. 1 The three stages of ion passing through the membrane. Stage 1 is the entering process of ions into the membrane, during which partial dehydration occurs. Stage 2 is the ion diffusion inside the membrane, during which ions may interact with functional groups on the membrane. Stage 3 is the returning of ions from the membrane to the solution on the other side, during which hydration of ions may occur.

Fig. 2 Schematic diagram of different driving forces corresponding to technology. (a) FO technology (osmotic pressure driving); (b) NF technology and RO technology (hydraulic driving); (c) ED technology (electric potential driving); (d) MCDI technology (electric potential driving).

Fig. 2(b), both NF and RO use a membrane to separate the left (permeation solution) and right (feed solution) solution.[47,49]

Applying hydraulic pressure above the right solution will cause the solute to pass through the membrane and enter the left

This journal is © The Royal Society of Chemistry 2024

Environ. Sci.: Water Res. Technol., 2024, **10**, 1305–1318 | **1307**

solution, which can only allow small molecular weight species to pass through.[50,51]

Electric potential driving corresponds to ED technology[52,31] and MCDI technology.[53] A schematic diagram of ED is shown in Fig. 2(c). The left and right sides of the device are electrode devices, which generate potential differences to separate anions and cations. AEM and CEM are employed in the tank. Upon application of voltage, the anions in the second tank will migrate to the left through AEM and enter the first tank, while the cations will migrate to the right through CEM and enter the third tank. Similarly, the anions in the fourth tank will migrate to the left and enter the third tank through AEM, while the cations will migrate to the right and enter the fifth tank through CEM. Finally, the solution in the second and fourth tank will be free of impurity ions.

A schematic diagram of MCDI technology is shown in Fig. 2(d). MCDI technology is commonly used in seawater desalination. In MCDI, AEM is installed near the positive electrode plate and CEM is placed near the negative electrode plate. After the saltwater passes through the electrode plate, the anions and cations in the saltwater migrate towards the upper and lower plates, respectively, due to electrostatic interaction.[54,55] Compared to general CDI technology, MCDI technology uses CEM and AEM to effectively prevent the adsorbed ions from being carried away by water flow. Moreover, it can also prevent the desorption ions from being readsorbed on the opposite electrode during the regeneration process.

The migration of ions from the solution to the channels also involves a process similar to concentration polarization in electrochemistry. There is an external concentration polarization phenomenon in the FO and RO processes.[56] The diffusion speed of ions from the solution to the channels is greater than the speed of ions entering the channels. As a result, ions will accumulate at the opening of channels. Consequently, there may be a difference between the ion concentration at the bulk phase of the solution and the opening of channels. Two different calculation methods for ion repulsion have been proposed. Ion repulsion is a measurable parameter to evaluate the selectivity of certain ions to pass through the membrane. The greater the ion repulsion of a membrane towards a certain ion, the less likely it is for that ion to pass through the membrane. Ion repulsion can be divided into observed ion repulsion (R_{obs}) and real ion repulsion (R_{real}). Between them, R_{obs} is based on the concentration of ions in the bulk phase of the solution, while R_{real} is based on the concentration of ions at the opening of channels. The calculation formula for the two ion repulsions is as follows:

$$\text{Observed ion repulsion: } R_{obs} = 1 - c_p/c_f \tag{1}$$

$$\text{Real ion repulsion: } R_{real} = 1 - c_p/c_m \tag{2}$$

where c_p is the concentration of a certain ion in the permeation solution, c_f is the concentration of a certain ion in the feed solution and c_m is the concentration of a certain ion at the opening of channels. c_m can be calculated from c_f.[57]

Ions are not electrically neutral, so they are surrounded by layers of solvent molecules in an aqueous environment.[58] For cations, a solvent layer is formed where the oxygen atoms in the water molecule face inward and the hydrogen atoms face outward. For anions, the situation is reversed. The concept of ion hydration radius has been proposed due to the presence of a solvent layer. During this process, the following factors will affect the entry of ions into the channels.

2.1.1. The hydration energy. Ions are surrounded by water molecules. As a consequence, they need to undergo a dehydration process to reduce their volume to pass through channels with a small size. The difficulty of the dehydration process will be closely related to the hydration energy of the ions due to the large differences in the hydration energies of different ions. Ions with high hydration energy are less likely to enter the channels. Ions with less negative hydration energy are prone to dehydration, resulting in smaller volumes and easier entry into channels. Hence, the difference in ion hydration energy allows ions to pass through membranes selectively.[59,60]

Lu et al. studied the selectivity of different cations passing through the MXene@PSS membrane (Fig. 3(a and b)).[61] In their work, the sizes of hydrated Li$^+$ and Mg^{2+} ions are 7.64 Å and 8.56 Å, respectively. Since the interlayer spacing of the membrane is 6 Å, the dehydration process should occur for ions to pass through the channels. Mg^{2+} (−1922 kJ mol^{-1}) has a more negative hydration energy than Li$^+$ (−515 kJ mol^{-1}). Thus, Mg^{2+} is less prone to dehydration and less likely to enter the channels. Therefore, a relatively high Li$^+$/Mg^{2+} selectivity of 28 was achieved. Li et al. also observed a similar separation efficiency of Li$^+$/Mg^{2+} by PEI/Cyclen-TMC (Fig. 3(c)).[62] Pang et al. used quaternization reaction to study the passage of Li$^+$ and Mg^{2+} through different hydrophobic membranes (Fig. 3(d)).[63] For membranes with different hydrophobicity, the experimental results show that the ion flux of Li$^+$ is greater than that of Mg^{2+}. The reason for this result is that the hydration energy of Mg^{2+} is more negative than that of Li$^+$. Liang et al. encapsulated sulfurized spiropyran (SSP) into ZIF-8 crystal and prepared a membrane to separate Li$^+$ ions from other cations (Fig. 3(e)).[64] The order of hydration strength is Mg^{2+} > Li$^+$ > Na$^+$ > K$^+$, which results in electrochemical impedance spectroscopy showing that the ion transfer resistance of Mg^{2+} is the highest and Mg^{2+} is the least likely to pass through the membrane. Wu et al. studied the separation of monovalent and multivalent metal ions through MOF (HKUST-1) channels (Fig. 3(f)).[65] In this study, the selectivity of the membrane for Li$^+$/Zr^{4+} can reach 3930 ± 373 owing to the more negative hydration energy and larger hydration diameter of Zr^{4+}.

2.1.2. The channel size and hydration radius. The size of channels can affect the passage of ions through them. Steric

1308 | Environ. Sci.: Water Res. Technol., 2024, 10, 1305–1318

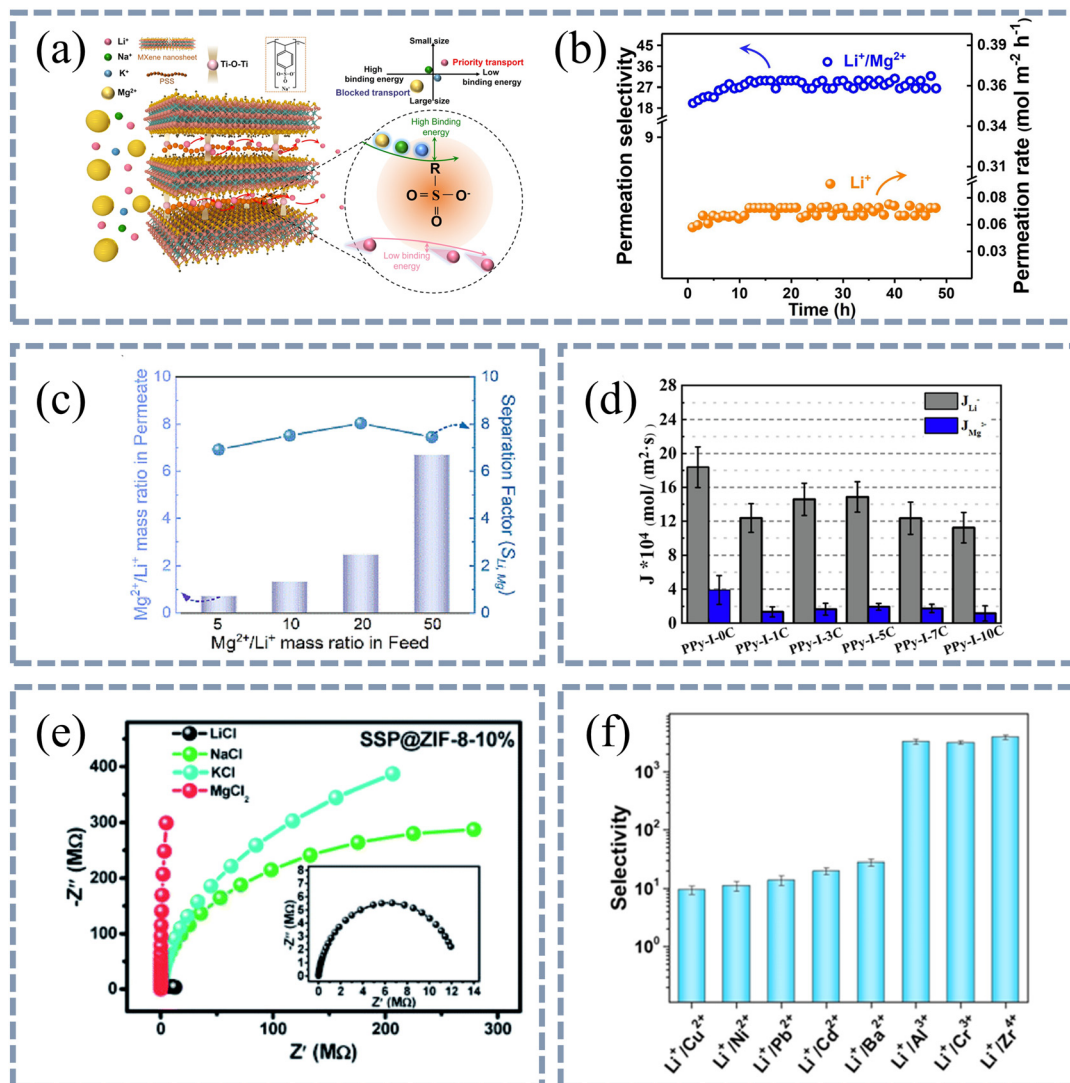This journal is © The Royal Society of Chemistry 2024

Fig. 3 The difference in hydration energy of ions results in selective passage of ions through the membranes. (a) Schematic diagram of channels for fast transport of Li$^+$ ions in MXene@PSS membranes. (b) Long-term stability of the MXene@PSS composite membrane. Li$^+$/Mg^{2+} permeation selectivity reaches 28 due to the more negative hydration energy of Mg^{2+} ions. Reproduced from ref. 61 with permission from John Wiley and Sons, copyright 2021. (c) Mg^{2+}/Li$^+$ mass ratio in the permeate and separation factor ($S_{Li,Mg}$) of PEI/Cyclen-TMC composite membrane with various Mg^{2+}/Li$^+$ mass ratios in the feed. $S_{Li,Mg}$ can reach 8.0 owing to the more negative hydration energy of Mg^{2+} ions. Reproduced from ref. 62 with permission from Elsevier, copyright 2023. (d) The flux of PPy–I–nC membranes in diffusion dialysis experiment of single salt after 1 h: Li$^+$ and Mg^{2+}. n in PPy–I–nC is the carbon chain length of the quaternary ammonium reagent used in the membrane preparation process. The flux of Li$^+$ ions is faster than that of Mg^{2+} ions because the hydration energy of lithium ions is less. Reproduced from ref. 63 with permission from Elsevier, copyright 2021. (e) Ion selectivity of the SSP@ZIF-8-10% membrane. The order of hydration strength is Mg^{2+} > Li$^+$ > Na$^+$ > K$^+$. Electrochemical impedance spectroscopy results show that the ion transfer resistance of Mg^{2+} is the largest. Reproduced from ref. 64 with permission from Royal Society of Chemistry, copyright 2020. (f) Ion selectivity of Li$^+$ to various metal ions of the MOF membrane. The selectivity of the membrane for Li$^+$/Zr^{4+} can reach 3930 ± 373 owing to the more negative hydration energy and larger hydration diameter of Zr^{4+}. Reproduced from ref. 65 with permission from John Wiley and Sons, copyright 2023.

effects will occur when they pass through the same channel because of different hydration and bare sizes of ions. According to the relative size between the channel size and the ion hydration size, the situation of ions passing through channels can be divided into three types:[66] (i) the channel size is greater than the hydration size of the ions. In this case, ions can enter the channels as a complete hydrated layer with the smallest energy barrier. (ii) The channel size is between the hydrated size of ions and that of bare ions. In this case, ions need to undergo partial dehydration to enter the channels, where the ions need to overcome a moderate energy barrier during the entering process. (iii) The bare size of ions is close to the channel size. In this case, the ions may undergo a deep dehydrating process, leading to the largest energy barrier when entering channels. Obviously, if the channel size is further reduced to be smaller than the bare size of the ions, the ions will not be able to pass through channels.

This journal is © The Royal Society of Chemistry 2024

Environ. Sci.: Water Res. Technol., 2024, **10**, 1305–1318 | **1309**

Based on the driving forces of ion dehydration, the existing research can be divided into two categories: (i) the ion dehydration is caused by steric effects between the hydrated ion and the channels of the membrane.[67,68] When the hydration size of an ion is greater than the size of the channel, the ion must reconstruct its solvent layer and undergo partial dehydration, where the coordinated water molecules in the hydration layer may decrease to reduce its hydration size. When the hydration size of the ion is smaller than the size of the channel, the ion can easily enter the channel without any dehydration. (ii) The ionic dehydration is caused by the decrease in environmental dielectric constant after ions enter the channel from the bulk phase. A

recently published study showed that in addition to steric effects, other factors can also affect ion dehydration. When the hydration size of ions is smaller than the channel size, dehydration may also occur (Fig. 4(a–d)).[69] Lu *et al.* used *in situ* TOF-SIMS technology to measure the number of water molecules coordinated with ions before and after they entered the channels. In their experiments, four membranes of NF90 (Fig. 4(a)), Trisep 1 (Fig. 4(b)), Trisep 2 (Fig. 4(c)), Trisep 3 (Fig. 4(d)) with the effective channel radius of 0.22 nm, 0.29 nm, 0.30 nm and 0.58 nm, respectively, were employed to understand the dehydration behavior of Na^+ (average hydration radius: 3.58 Å). From the perspective of steric effect alone, Na^+ ions will undergo dehydration
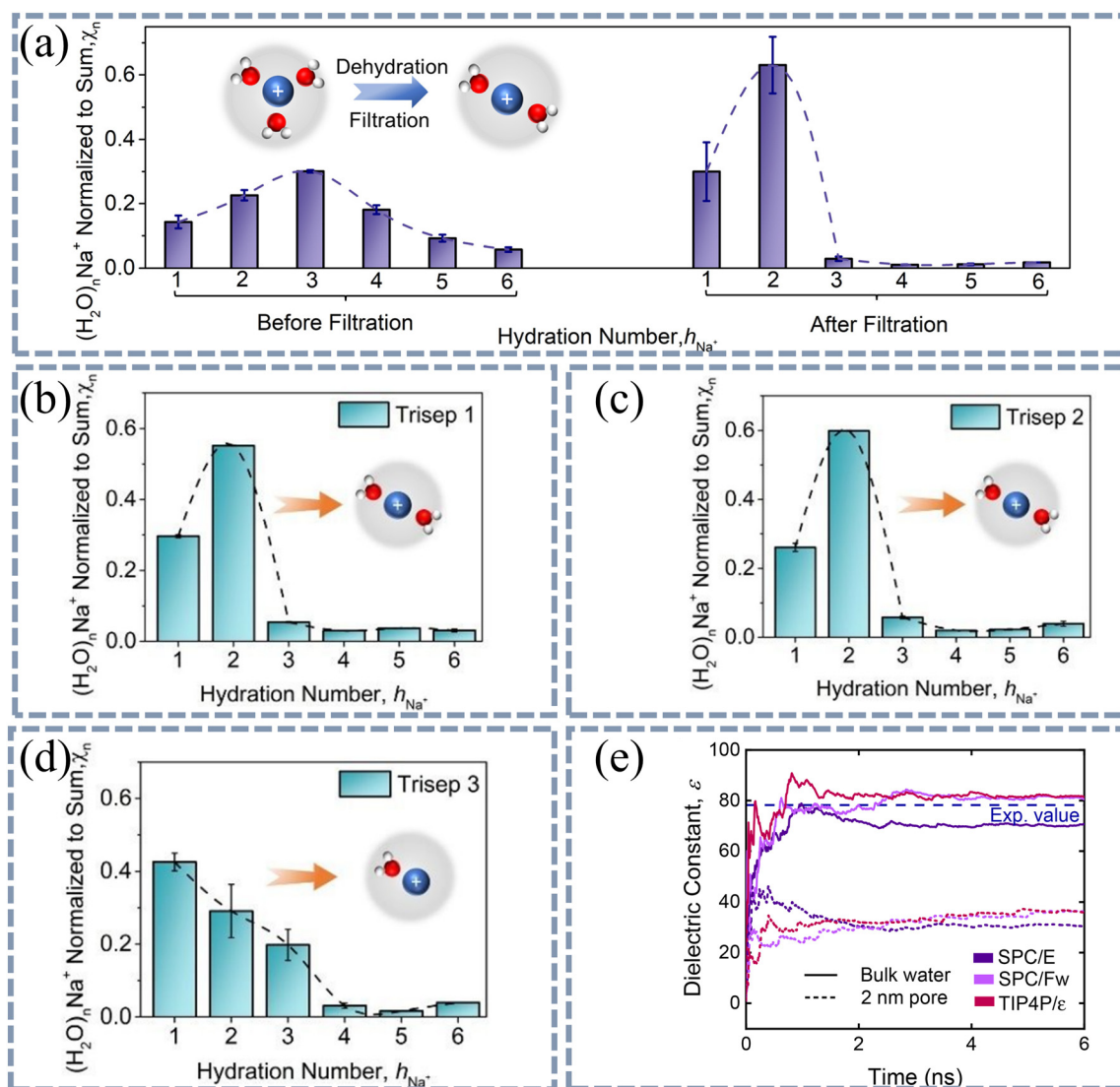

Fig. 4 Steric effects or dielectric effects lead to dehydration of ions. (a) Variation of hydration number (h_{Na^+}) of Na^+ ions before and after filtration of 10 mM NaCl solutions by NF90 (effective channel radius: 0.22 nm). h_{Na^+} of Na^+ ions after filtration of 10 mM NaCl solution by (b) Trisep 1 (effective channel radius: 0.29 nm), (c) Trisep 2 (effective channel radius: 0.30 nm), and (d) Trisep 3 (effective channel radius: 0.58 nm). Dehydration occurs when Na^+ ions pass through all four membranes. Reproduced from ref. 69 with permission from American Chemical Society, copyright 2021. (e) MD simulations of the dielectric constant of bulk and nanoconfined water by the rigid three-site SPC/E, flexible three-site SPC/Fw, and rigid four-site TIP4P/ε water models. For bulk water, the dielectric constant is ~80. For water molecules in 2 nm pores, the dielectric constant is ~30.

1310 | *Environ. Sci.: Water Res. Technol.*, 2024, **10**, 1305–1318

This journal is © The Royal Society of Chemistry 2024

through NF90, Trisep 1 and Trisep 2 membranes, while dehydration will not occur through Trisep 3 membranes. When Na^+ ions pass through NF90, Trisep 1 and Trisep 2 membranes, the proportion of Na^+ coordinated with 3 water molecules significantly decreases from 0.3 to 0.03, 0.05 and 0.07, respectively. This confirms that Na^+ will undergo dehydration through NF90, Trisep 1 and Trisep 2 membranes. However, the experimental results also showed that the proportion of 3 coordinated Na^+ decreased to 0.28 after passing through Trisep 3 membrane, suggesting that even in the absence of steric effects, ions may undergo dehydration through the channels.

It is believed that the dehydration in large channels is caused by the confinement effect due to the low dielectric constant inside the channels. Ritt *et al.* used molecular dynamics simulations to obtain the dielectric constant of water molecules in bulk and in 2 nm pores (Fig. 4(e)).[70] This indicates that water in the pores exhibits a lower dielectric constant compared to bulk water. Epsztein *et al.* also mentioned the reasons for this dehydration in their study.[36] At present, it has been experimentally[71,72] and theoretically[73,74] proven that water molecules at the interface exhibit layered structures. The dipole orientations of layered water molecules are rearranged at the interface between the channel wall and the solution phase. The directional arrangement of these dipoles is relatively stable, even when an external electric field is applied. Therefore, these layered water molecules on the surface exhibit a very low polarizability.[75] The low polarization of water molecules reduces the hydration energy of ions, leading to dehydration when ions enter the channels.

2.1.3. The charge of ions. The charge of ions can also affect the selective passage of ions through channels *via* electrostatic interactions.[76,77] If the channel carries the same charge as the ion, the strong electrostatic repulsion between the channel and the ion would prevent the ion from entering the channel. In contrast, when the channel wall and ions have opposite charges, the entrance process of ions into the channel could be significantly promoted.

2.2. Ion migration in the membrane

Regarding free ions in the solution, the chemical environment around the ions will undergo significant changes after entering the channels. In particular, in small channels, ions are likely to interact with the inner wall of the channel, thereby affecting the selective permeability of the membrane to different ions.[78,79] The following focuses on the main issues influencing ion migration in the membrane, such as the charge of ions, the length and size of channels, and the interaction between the groups in the channel and the ion.

2.2.1. The charge of ions. The type of charge carried by ions affects not only the entry of ions into the channels in the first stage but also the diffusion of ions within the channels in the second stage. For ions with the same charge as the channel, ions are less likely to enter the channels due

to electrostatic repulsion, which lowers their diffusion barrier. In contrast, if the ion carries different charges from that of the groups of channels, it would be strongly attracted by the wall group of channels, leading to facile entrance in the channel openings but slow diffusion inside channels. Therefore, the apparent ion selectivity is a comprehensive reflection of these two processes. Labbez *et al.* summarized two types of retention (*i.e.* ion repulsion) behaviors, the quasi-symmetric curves and the asymmetric S-shaped curves, in the nanofiltration process at different pH values (Fig. 5(a)).[80] Quasi-symmetric curves are suitable for symmetric salts such as KCl, LiCl and $MgSO_4$, while asymmetric S-shaped curves are suitable for asymmetric salts such as K_2SO_4 and $MgCl_2$. For symmetric salts, the channel walls are positively charged at low pH and are repulsive to cations. At high pH, the channel walls are negatively charged and are repulsive to anions. When the pH is close to the isoelectric point (IEP) of the channel wall, the channels are almost uncharged, leading to significantly reduced repulsion to both anions and cations. However, the retention is determined by the ions with higher valence in the asymmetric salt (for example, SO_4^{2-} in K_2SO_4, Mg^{2+} in
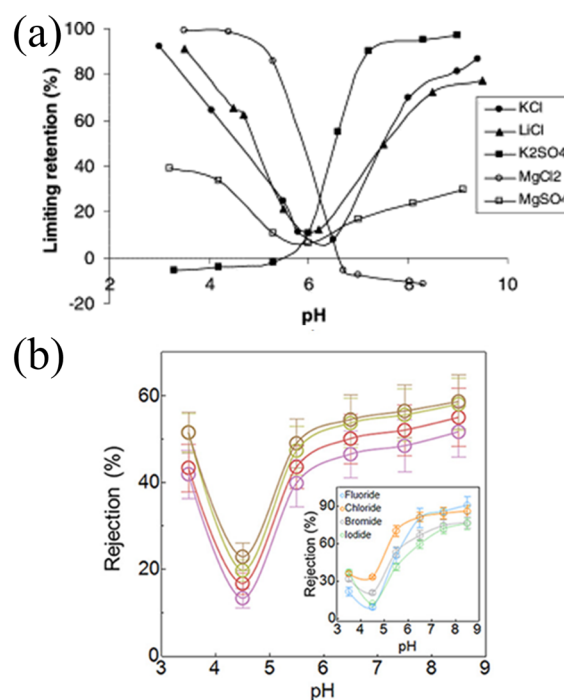

Fig. 5 The effect of charge carried by ions on their passage through pores. (a) Relationship curve of retention with pH change during the nanofiltration process. There are two types of retention behaviors, the quasi-symmetric curves (KCl, LiCl and $MgSO_4$) and the asymmetric S-shaped curves (K_2SO_4 and $MgCl_2$). Reproduced from ref. 80 with permission from Elsevier, copyright 2002. (b) Relationship between ion rejection of LiCl (purple), NaCl (red), KCl (olive green), and CsCl (brown) through a polyamide membrane and pH changes. Inset: rejection of monovalent anions-fluoride (blue), chloride (orange), bromide (gray), and iodide (green), as sodium salts-at different pH values. All curves exhibit the characteristics of the quasi-symmetric curve. Reproduced from ref. 81 with permission from American Chemical Society, copyright 2021.

This journal is © The Royal Society of Chemistry 2024

Environ. Sci.: Water Res. Technol., 2024, **10**, 1305–1318 | **1311**

MgCl$_2$). For instance, the retention of K$_2$SO$_4$ is determined by SO$_4^{2-}$, which would obviously increase the retention at high pH values by the strong repulsion toward the negatively charged channels. The same conclusion was also validated in Shefer's study.[81] Fig. 5(b) shows the relationship between ion repulsion of LiCl (purple), NaCl (red), KCl (olive green) and CsCl (brown) under various pH values. Typical quasi-symmetric curves with the IEP of ~4.5 were observed for all the above symmetric salts.

2.2.2. The interaction between groups on the channel wall and ions. Similar to the groups at the channel opening, the channel wall groups will also interact with ions. Therefore, strong ion–group interactions will cause the ions to be firmly anchored by the channel wall, which in turn reduces the ion transportation rate in the channels. Sheng *et al.* investigated the permeation rate and selectivity between K$^+$ and Mg^{2+} on the TpBDMe$_2$ membrane (Fig. 6(a–c)).[82] Because of the strong affinity between Mg^{2+} and the channel wall, a relatively small permeation rate of Mg^{2+} was observed with a high K$^+$/Mg^{2+} selectivity of 1000. Guo *et al.* studied the selective passage of Li$^+$ ions through a membrane made by adding polystyrene sulfonate to HKUST-1 MOF material (Fig. 6(d and e)).[83] Since
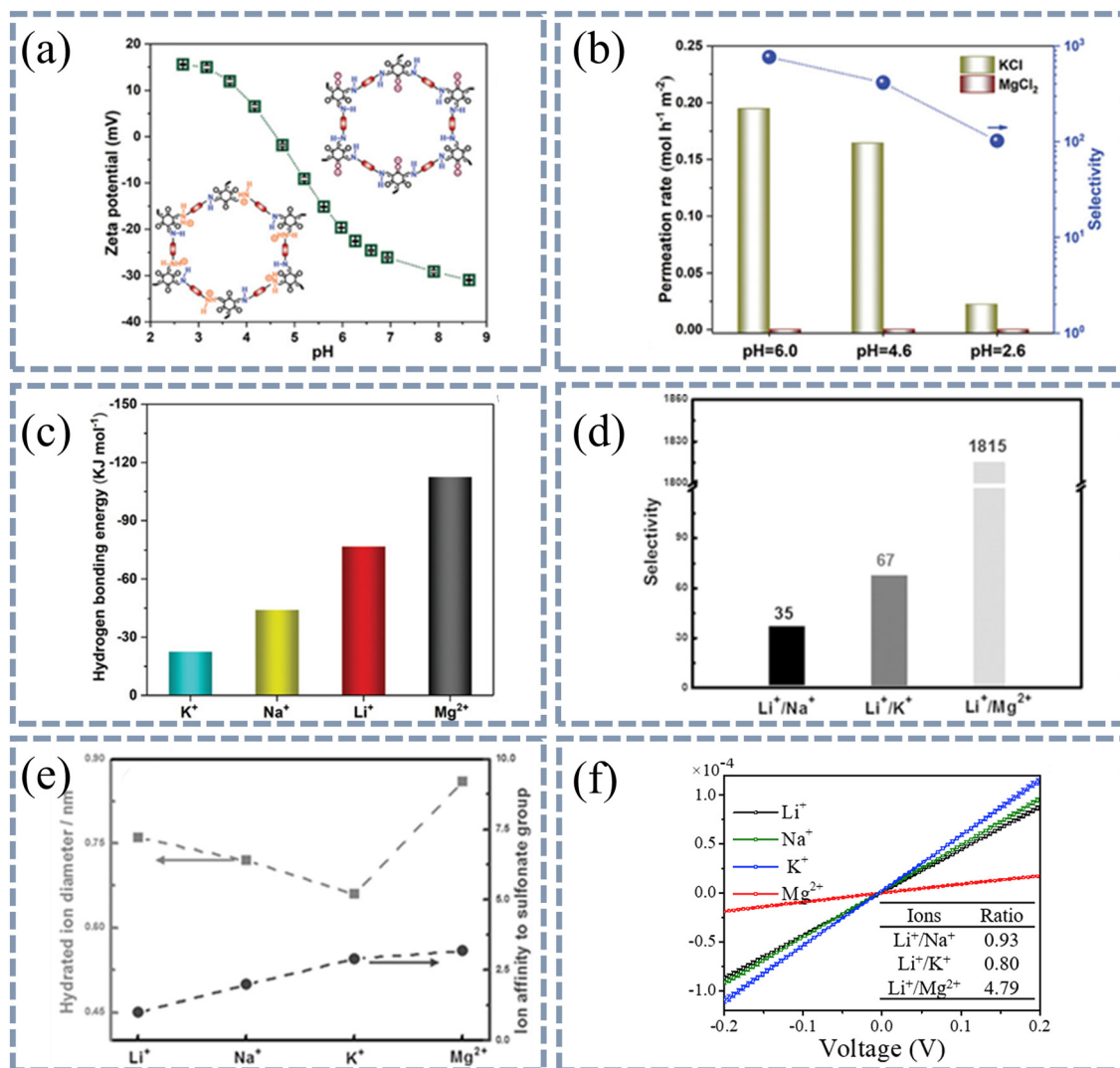

Fig. 6 The interaction between groups on the channel wall and ions affects the transport of ions in the membrane. (a) Zeta potential of TpBDMe$_2$ membranes as a function of pH. (b) Effects of pH on mono-/divalent cation permeation rate and selectivity of TpBDMe$_2$ membranes. (c) The hydrogen bonding energy between hydrated ions and the channel wall of TpBDMe$_2$ membranes. Because of the strong affinity between Mg^{2+} and the channel wall, a relatively low permeation rate of Mg^{2+} was observed with a high K$^+$/Mg^{2+} selectivity of 1000. Reproduced from ref. 82 with permission from John Wiley and Sons, copyright 2021. (d) Binary ion selectivity of PSS@HKUST-1-6.7 in 0.5 M LiCl and 0.5 M M^{n+}Cl$_n$ electrolytes. (e) Relative strength of affinity between sulfonated group and ions (circles) and the hydrated ion diameters (squares). The selectivity of Li$^+$/Na$^+$, Li$^+$/K$^+$, and Li$^+$/Mg^{2+} can reach 35, 67, and 1825, respectively, because the binding affinity between ions and the sulfonic group follow the sequence Mg^{2+} > K$^+$ > Na$^+$ > Li$^+$. Reproduced from ref. 83 with permission from John Wiley and Sons, copyright 2016. (f) I–V curves of HSO$_3$-UiO-66-0.6@PVC membranes. The strong affinity between Mg^{2+} and –SO$_3$– results in the highest separation ratio of Li$^+$/Mg^{2+}. Reproduced from ref. 84 with permission from Elsevier, copyright 2020.

the binding affinity between ions and sulfonic groups follow the sequence $Mg^{2+} > K^+ > Na^+ > Li^+$, the selectivity of Li^+/Na^+, Li^+/K^+, and Li^+/Mg^{2+} can reach 35, 67, and 1815, respectively. Here, the HKUST-1 MOF not only acts as a carrier for sulfonate groups but also provides an appropriate channel to sieve ions. Zhang *et al.* studied the separation performance of six PVC-based hybrid membranes containing metal organic frameworks for Li^+ ions and Mg^{2+} ions (Fig. 6(f)).[84] Compared to other membranes, the HSO_3-UiO-66-0.6@PVC membrane with rich $-SO_3^-$ groups on the channel wall exhibits the highest separation ratio of Li^+/Mg^{2+} due to the strong affinity between Mg^{2+} and $-SO_3^-$, which decreases the diffusion rate of Mg^{2+} ions in the membrane.

2.2.3. The length and size of the channel. The channel geometry, including the length and size of the channel, will also significantly affect the diffusion behavior of ions. Generally, the longer the channel, the better the partitioning of different ions, which results in superior selectivity of the membrane. Wang *et al.* investigated the effect of channel length on ion permeation rate and ion selectivity in COF membranes.[85] As shown in Fig. 7(a), as the length of the channel increases, the permeation rates of both K^+ ions and Li^+ ions decrease, while the selectivity increases from 13.5 to 16.8.

For the channel size, it affects not only the entering process of ions in the channel opening but also their transportation inside the channels. When the channel wall is charged with a

Fig. 7 The length and size of the channel affect the transport of ions in the membrane. (a) Transport performances of COF membranes under different stage numbers. As the stage number increases, the permeation rates of both K^+ and Li^+ ions decrease, while the selectivity increases from 13.5 to 16.8. (b) Schematic diagram of double layer model. The side near the interface is the Stern layer and that on the side away from the interface is the diffusion layer. (c) Double layer may not overlap when the ion concentration is low. (d) Double layer may overlap when the ion concentration is high. Reproduced from ref. 86 with permission from Royal Society of Chemistry, copyright 2022. (e) Schematic diagram of PET/MIL-53-COOH NC structure. (f) Asymmetrical *I–V* curves of 0.1 M LiCl, NaCl, KCl, and HCl in PET/MIL-53-COOH NC. The rectification effect occurs due to the overlap of the double layer.

This journal is © The Royal Society of Chemistry 2024

Environ. Sci.: Water Res. Technol., 2024, **10**, 1305–1318 | **1313**

certain amount of positive or negative charges, a double layer structure will form near the channel wall. According to the Stern model, the double layer is divided into the Stern layer and the diffusion layer (Fig. 7(b)). In the Stern layer, the surface charge of the channel wall would strongly attract the counter ions, forming a stable adsorption layer on the channel wall. However, beyond the Stern layer, the diffusion layer may consist of both cations and anions, which do not directly interact with the channel wall and are weakly affected by the electrostatic attraction or repulsion of the channel wall. As a result, the Stern layer of the channel usually exhibits much better selectivity than the diffusion layer. When the channel size reduces to a certain size where the Stern layers on both sides overlap each other, the selectivity towards counter ions could be significantly improved. Therefore, if the Stern layers on both sides of the channel overlap, there is selective passage of anions and cations through the channels (Fig. 7(c and d)).[86] The thickness of the Stern layer is very similar to the Debye shielding length (λ_D).[87] According to relevant literature reports, the thickness of the Stern layer is also sensitive to the ion concentration in the solution, where a high ion concentration should result in a thin Stern layer.[88,89,86]

Lu *et al.* studied the rectification effect of alkali metal ions in PET/MIL-53-COOH nanochannels with a unique base–tip structure (Fig. 7(e and f)),[90] where the tip side is filled by the MIL-53 MOF with a channel size of 8.1 Å. For all the three salts (*i.e.* LiCl, NaCl and KCl), the diffusion current could be detected only when a reverse voltage is applied, suggesting that Li^+, Na^+ and K^+ ions can migrate only from tip to base. In fact, when a reverse voltage is applied, the cation migration from tip to base is driven by both the potential gradient and the concentration gradient. Meanwhile, the anions may migrate from base to tip in the presence of an electric field. However, due to the overlap of the double layers at the tip, the anions cannot pass through the channels at the tip side, leading to the accumulation of anions at the base. Moreover, to balance the charge, more cations will enter the base side, and the cation diffusion from tip to base is further promoted. When a forward voltage is applied, the potential gradient of the cations is opposite to the concentration gradient, resulting in a much smaller number of migrated cations. For anions, the overlapped double electric layers at the tip would also prevent the anion diffusion from tip to base. Therefore, no diffusion current could be observed with a forward voltage.

Conclusions

The ion diffusion mechanism in the membrane separation process is summarized in this review. It should be noted that although the ion diffusion is divided into three stages, the influences of the above issues might be observed throughout the entire membrane separation process. Most studies that achieve ion selectivity through channels mainly focus on (i) the difference in dehydration process when ions enter the channels, where only the ions with small dehydration energies are allowed, and (ii) the difference in the interaction

between ions and channel wall groups. The reason why some ions can freely migrate within the channel, while others are anchored near the groups on the channel wall, could be attributed to the different bonding energies between different ions and groups on the channel wall.

At present, the main problems faced by using membrane technology to achieve ion selectivity through channels are (i) the inability to ensure good permeation flux while maintaining high ion selectivity, *i.e.* the trade-off between permeation and selectivity. The ideal membrane should have abundant channels with a narrow channel size distribution and the desired functional groups on the channel wall surface.[91] The design and development of new membrane fabrication technologies should be a promising approach to tackle the above contradictions. (ii) The existing techniques cannot effectively measure the migration of ions in channels due to the limitations of temporal and spatial resolution.[92] In order to further understand the ion transportation mechanism, researchers should first make good use of computational modelling, such as molecular dynamics simulation and density functional theory calculation. Secondly, relevant testing techniques should be further developed to meet the needs of *in situ* measurement during the membrane separation.[69] (iii) The stability of the membrane should be further improved. A series of materials, such as MOFs,[23] COFs,[93] MXene[94] and graphite oxides,[95] are employed to prepare membranes with superior structural and chemical stability. For MOFs and COFs, researchers should pay attention to the impact of defects on membrane performance. For MXene and graphite oxides, more attention should be paid to the influence of interlayer spacing expansion on membrane performance after immersion in the solution.

Author contributions

Jian Zhang: writing – original draft. Qiang Gao: conceptualization. Bo Han: writing – review & editing. Chenggang Zhou: funding acquisition.

Conflicts of interest

There are no conflicts to declare.

Acknowledgements

References

1 J. Liu, H. Ma, Z. Wen, H. Li, J. Yang, N. Pei, P. Zhang and J. Zhao, Layered Ag-graphene films synthesized by Gamma ray irradiation for stable lithium metal anodes in carbonate-based electrolytes, *J. Energy Chem.*, 2022, **64**, 354–363.

2 Y. Zhang, Y. Liu, Z. Liu, X. Wu, Y. Wen, H. Chen, X. Ni, G. Liu, J. Huang and S. Peng, MnO2 cathode materials with the improved stability via nitrogen doping for aqueous zinc-ion batteries, *J. Energy Chem.*, 2022, **64**, 23–32.

3 T. Raj, K. Chandrasekhar, A. N. Kumar, P. Sharma, A. Pandey, M. Jang, B. H. Jeon, S. Varjani and S. H. Kim, Recycling of cathode material from spent lithium-ion batteries: Challenges and future perspectives, *J. Hazard. Mater.*, 2022, **429**, 128312.

4 H. Vikström, S. Davidsson and M. Höök, Lithium availability and future production outlooks, *Appl. Energy*, 2013, **110**, 252–266.

5 J. Hou, H. Zhang, A. W. Thornton, A. J. Hill, H. Wang and K. Konstas, Lithium extraction by emerging metal–organic framework-based membranes, *Adv. Funct. Mater.*, 2021, **31**(46), 2105991.

6 S. Lei, W. Sun and Y. Yang, Solvent extraction for recycling of spent lithium-ion batteries, *J. Hazard. Mater.*, 2022, **424**, 127654.

7 Y. Zhang, Y. Hu, L. Wang and W. Sun, Systematic review of lithium extraction from salt-lake brines via precipitation approaches, *Miner. Eng.*, 2019, **139**, 105868.

8 N. Um and T. Hirato, in *Zero-Carbon Energy Kyoto 2012*, 2013, ch. 16, pp. 149–154, DOI: **10.1007/978-4-431-54264-3_16**.

9 G. Zante, A. Masmoudi, R. Barillon, D. Trébouet and M. Boltoeva, Separation of lithium, cobalt and nickel from spent lithium-ion batteries using TBP and imidazolium-based ionic liquids, *J. Ind. Eng. Chem.*, 2020, **82**, 269–277.

10 Y. Luo, C. Yin and L. Ou, Recycling of waste lithium-ion batteries via a one-step process using a novel deep eutectic solvent, *Sci. Total Environ.*, 2023, **902**, 166095.

11 P.-Y. Ji, Z.-Y. Ji, Q.-B. Chen, J. Liu, Y.-Y. Zhao, S.-Z. Wang, F. Li and J.-S. Yuan, Effect of coexisting ions on recovering lithium from high Mg2+/Li+ ratio brines by selective-electrodialysis, *Sep. Purif. Technol.*, 2018, **207**, 1–11.

12 Q. Wang, Y. Wang, Y. Huang, H. Wang, Y. Gao, M. Zhao, L. Tu, L. Xue and C. Gao, Polyethyleneimine (PEI) based positively charged thin film composite polyamide (TFC-PA) nanofiltration (NF) membranes for effective Mg2+/Li+ separation, *Desalination*, 2023, **565**, 116814.

13 A. Alsabbagh, S. Aljarrah and M. Almahasneh, Lithium enrichment optimization from Dead Sea end brine by chemical precipitation technique, *Miner. Eng.*, 2021, **170**, 107038.

14 A. Masmoudi, G. Zante, D. Trébouet, R. Barillon and M. Boltoeva, Solvent extraction of lithium ions using benzoyltrifluoroacetone in new solvents, *Sep. Purif. Technol.*, 2021, **255**, 117653.

15 J. R. Werber, C. O. Osuji and M. Elimelech, Materials for next-generation desalination and water purification membranes, *Nat. Rev. Mater.*, 2016, **1**(5), 1–15.

16 J. Zhang, X. Cui, F. Yang, L. Qu, F. Du, H. Zhang and J. Wang, Hybrid cation exchange membranes with lithium ion-sieves for highly enhanced Li+ permeation and permselectivity, *Macromol. Mater. Eng.*, 2019, **304**(1), 1800567.

17 R. M. DuChanois, N. J. Cooper, B. Lee, S. K. Patel, L. Mazurowski, T. E. Graedel and M. Elimelech, Prospects of metal recovery from wastewater and brine, *Nat. Water.*, 2023, **1**, 37–46.

18 N. R. Aluru, F. Aydin, M. Z. Bazant, D. Blankschtein, A. H. Brozena, J. P. de Souza, M. Elimelech, S. Faucher, J. T. Fourkas, V. B. Koman, M. Kuehne, H. J. Kulik, H. K. Li, Y. Li, Z. Li, A. Majumdar, J. Martis, R. P. Misra, A. Noy, T. A. Pham, H. Qu, A. Rayabharam, M. A. Reed, C. L. Ritt, E. Schwegler, Z. Siwy, M. S. Strano, Y. Wang, Y. C. Yao, C. Zhan and Z. Zhang, Fluids and electrolytes under confinement in single-digit nanopores, *Chem. Rev.*, 2023, **123**(6), 2737–2831.

19 X. Lu and M. Elimelech, Fabrication of desalination membranes by interfacial polymerization: history, current efforts, and future directions, *Chem. Soc. Rev.*, 2021, **50**, 6290–6307.

20 C. Ji, Z. Zhai, C. Jiang, P. Hu, S. Zhao, S. Xue, Z. Yang, T. He and Q. J. Niu, Recent advances in high-performance TFC membranes: A review of the functional interlayers, *Desalination*, 2021, **500**, 114869.

21 M. Wang, Y. Wang, J. Zhao, J. Zou, X. Liang, Z. Zhu, J. Zhu, H. Wang, Y. Wang, F. Pan and Z. Jiang, Electrochemical Interfacial Polymerization toward Ultrathin COF Membranes for Brine Desalination, *Angew. Chem.*, 2023, **62**, e202219084.

22 H. Qi, Y. Peng, X. Lv, F. Xu, B. Su and L. Han, Synergetic effects of COFs interlayer regulation and surface modification on thin-film nanocomposite reverse osmosis membrane with high performance, *Desalination*, 2023, **548**, 116265.

23 S. Raggam, M. Mohammad, Y. Choo, G. Naidu, M. Zargar, H. K. Shon and A. Razmjou, Advances in metal organic framework (MOF)–Based membranes and adsorbents for lithium-ion extraction, *Sep. Purif. Technol.*, 2023, **307**, 122628.

24 W. Suwaileh, N. Pathak, H. Shon and N. Hilal, Forward osmosis membranes and processes: A comprehensive review of research trends and future outlook, *Desalination*, 2020, **485**, 114455.

25 D. L. Shaffer, J. R. Werber, H. Jaramillo, S. Lin and M. Elimelech, Forward osmosis: Where are we now?, *Desalination*, 2015, **356**, 271–284.

26 A. W. Mohammad, Y. H. Teow, W. L. Ang, Y. T. Chung, D. L. Oatley-Radcliffe and N. Hilal, Nanofiltration membranes review: Recent advances and future prospects, *Desalination*, 2015, **356**, 226–254.

27 D. L. Oatley-Radcliffe, M. Walters, T. J. Ainscough, P. M. Williams, A. W. Mohammad and N. Hilal, Nanofiltration membranes and processes: A review of research trends over the past decade, *J. Water Process Eng.*, 2017, **19**, 164–171.

28 S. Zhao, Z. Liao, A. Fane, J. Li, C. Tang, C. Zheng, J. Lin and L. Kong, Engineering antifouling reverse osmosis membranes: A review, *Desalination*, 2021, **499**, 114857.

29 Y. J. Lim, K. Goh, M. Kurihara and R. Wang, Seawater desalination by reverse osmosis: Current development and future challenges in membrane fabrication–A review, *J. Membr. Sci.*, 2021, **629**, 119292.

This journal is © The Royal Society of Chemistry 2024

Environ. Sci.: Water Res. Technol., 2024, **10**, 1305–1318 | **1315**

30 J. M. A. Juve, F. M. S. Christensen, Y. Wang and Z. Wei, Electrodialysis for metal removal and recovery: A review, *Chem. Eng. J.*, 2022, **435**, 134857.

31 S. Al-Amshawee, M. Y. B. M. Yunus, A. A. M. Azoddein, D. G. Hassell, I. H. Dakhil and H. A. Hasan, Electrodialysis desalination for water and wastewater: A review, *Chem. Eng. J.*, 2020, **380**, 122231.

32 P. M. Biesheuvel and A. van der Wal, Membrane capacitive deionization, *J. Membr. Sci.*, 2010, **346**, 256–262.

33 L. Wang and S. Lin, Mechanism of Selective Ion Removal in Membrane Capacitive Deionization for Water Softening, *Environ. Sci. Technol.*, 2019, **53**, 5797–5804.

34 X. Li, Y. Mo, W. Qing, S. Shao, C. Y. Tang and J. Li, Membrane-based technologies for lithium recovery from water lithium resources: A review, *J. Membr. Sci.*, 2019, **591**, 117317.

35 R. Wang, R. Alghanayem and S. Lin, Multipass Nanofiltration for Lithium Separation with High Selectivity and Recovery, *Environ. Sci. Technol.*, 2023, **57**, 14464–14471.

36 R. Epsztein, R. M. DuChanois, C. L. Ritt, A. Noy and M. Elimelech, Towards single-species selectivity of membranes with subnanometre pores, *Nat. Nanotechnol.*, 2020, **15**, 426–436.

37 S. Sahu, M. Di Ventra and M. Zwolak, Dehydration as a Universal Mechanism for Ion Selectivity in Graphene and Other Atomically Thin Pores, *Nano Lett.*, 2017, **17**, 4719–4724.

38 A. A. Uliana, N. T. Bui, J. Kamcev, M. K. Taylor, J. J. Urban and J. R. Long, Ion-capture electrodialysis using multifunctional adsorptive membranes, *Science*, 2021, **372**, 296–299.

39 P. Zuo, C. Ye, Z. Jiao, J. Luo, J. Fang, U. S. Schubert, N. B. McKeown, T. L. Liu, Z. Yang and T. Xu, Near-frictionless ion transport within triazine framework membranes, *Nature*, 2023, 1–7, DOI: **10.1038/s41586-023-05888-x**.

40 K. Zhou and Z. P. Xu, Ion Permeability and Selectivity in Composite Nanochannels: Engineering through the End Effects, *J. Phys. Chem. C*, 2020, **124**, 4890–4898.

41 R. Wang and S. Lin, Pore model for nanofiltration: History, theoretical framework, key predictions, limitations, and prospects, *J. Membr. Sci.*, 2021, **620**, 118809.

42 R. M. DuChanois, C. J. Porter, C. Violet, R. Verduzco and M. Elimelech, Membrane Materials for Selective Ion Separations at the Water-Energy Nexus, *Adv. Mater.*, 2021, **33**, e2101312.

43 M. T. Pham, S. Nishihama and K. Yoshizuka, Concentration of lithium by forward osmosis, *Hydrometallurgy*, 2020, **197**, 105485.

44 M. Al-Furaiji, M. Kadhom, K. Kalash, B. Waisi and N. Albayati, Preparation of thin-film composite membranes supported with electrospun nanofibers for desalination by forward osmosis, *Drinking Water Eng. Sci.*, 2020, **13**, 51–57.

45 M. Al-Furaiji, B. Waisi, K. Kalash and M. Kadhom, Effect of polymer substrate on the performance of thin-film composite nanofiltration membranes, *Int. J. Polym. Anal. Charact.*, 2022, **27**, 316–325.

46 J. Luo and Y. Wan, Effect of highly concentrated salt on retention of organic solutes by nanofiltration polymeric membranes, *J. Membr. Sci.*, 2011, **372**, 145–153.

47 N. Hilal, H. Al-Zoubi, N. A. Darwish, A. W. Mohamma and M. Abu Arabi, A comprehensive review of nanofiltration membranes:Treatment, pretreatment, modelling, and atomic force microscopy, *Desalination*, 2004, **170**, 281–308.

48 B. Hua, H. Xiong, M. Kadhom, L. Wang, G. Zhu, J. Yang, G. Cunningham and B. Deng, Physico-Chemical Processes, *Water Environ. Res.*, 2017, **89**, 974–1028.

49 G. Amy, N. Ghaffour, Z. Li, L. Francis, R. V. Linares, T. Missimer and S. Lattemann, Membrane-based seawater desalination: Present and future prospects, *Desalination*, 2017, **401**, 16–21.

50 H. Zhang, Q. He, J. Luo, Y. Wan and S. B. Darling, Sharpening Nanofiltration: Strategies for Enhanced Membrane Selectivity, *ACS Appl. Mater. Interfaces*, 2020, **12**, 39948–39966.

51 P. M. Biesheuvel, S. Porada, M. Elimelech and J. E. Dykstra, Tutorial review of reverse osmosis and electrodialysis, *J. Membr. Sci.*, 2022, **647**, 120221.

52 A. Campione, L. Gurreri, M. Ciofalo, G. Micale, A. Tamburini and A. Cipollina, Electrodialysis for water desalination: A critical assessment of recent developments on process fundamentals, models and applications, *Desalination*, 2018, **434**, 121–160.

53 S. Porada, R. Zhao, A. van der Wal, V. Presser and P. M. Biesheuvel, Review on the science and technology of water desalination by capacitive deionization, *Prog. Mater. Sci.*, 2013, **58**, 1388–1442.

54 P. Liu, T. Yan, L. Shi, H. S. Park, X. Chen, Z. Zhao and D. Zhang, Graphene-based materials for capacitive deionization, *J. Mater. Chem. A*, 2017, **5**, 13907–13943.

55 Y. M. Volfkovich, Capacitive Deionization of Water (A Review), *Russ. J. Electrochem.*, 2020, **56**, 18–51.

56 J. Wang, D. S. Dlamini, A. K. Mishra, M. T. M. Pendergast, M. C. Y. Wong, B. B. Mamba, V. Freger, A. R. D. Verliefde and E. M. V. Hoek, A critical review of transport through osmotic membranes, *J. Membr. Sci.*, 2014, **454**, 516–537.

57 X. Zhai, Y. L. Wang, R. Dai, X. Li and Z. Wang, Roles of Anion-Cation Coupling Transport and Dehydration-Induced Ion-Membrane Interaction in Precise Separation of Ions by Nanofiltration Membranes, *Environ. Sci. Technol.*, 2022, **56**, 14069–14079.

58 B. Corry, Mechanisms of selective ion transport and salt rejection in carbon nanostructures, *MRS Bull.*, 2017, **42**, 306–310.

59 B. Tansel, Significance of thermodynamic and physical characteristics on permeation of ions during membrane separation: Hydrated radius, hydration free energy and viscous effects, *Sep. Purif. Technol.*, 2012, **86**, 119–126.

60 L. A. Richards, B. S. Richards, B. Corry and A. I. Schafer, Experimental energy barriers to anions transporting through nanofiltration membranes, *Environ. Sci. Technol.*, 2013, **47**, 1968–1976.

61 Z. Lu, Y. Wu, L. Ding, Y. Wei and H. Wang, A Lamellar MXene (Ti3 C2 Tx)/PSS Composite Membrane for Fast and Selective Lithium-Ion Separation, *Angew. Chem.*, 2021, **60**, 22265–22269.

1316 | *Environ. Sci.: Water Res. Technol.*, 2024, **10**, 1305–1318

This journal is © The Royal Society of Chemistry 2024

62 T. Li, X. Zhang, Y. Zhang, J. Wang, Z. Wang and S. Zhao, Nanofiltration membrane comprising structural regulator Cyclen for efficient Li+/Mg2+ separation, *Desalination*, 2023, **556**, 116575.

63 X. Pang, X. Yu, Y. He, S. Dong, X. Zhao, J. Pan, R. Zhang and L. Liu, Preparation of monovalent cation perm-selective membranes by controlling surface hydration energy barrier, *Sep. Purif. Technol.*, 2021, **270**, 118768.

64 H.-Q. Liang, Y. Guo, X. Peng and B. Chen, Light-gated cation-selective transport in metal–organic framework membranes, *J. Mater. Chem. A*, 2020, **8**, 11399–11405.

65 Z. Wu, C. Li, C. Huang, S. Cheng, X. Ouyang, W. Chen, P. Zhang, Y. Jiang and L. Jiang, Wettability-Regulated Synthesis of Metal-Organic Framework Array with Subnanochannels Enables Efficient Separation of Mono–/Multivalent Metal Ions, *Chemistry*, 2023, e202301163, DOI: **10.1002/chem.202301163**.

66 L. A. Richards, A. I. Schafer, B. S. Richards and B. Corry, Quantifying barriers to monovalent anion transport in narrow non-polar pores, *Phys. Chem. Chem. Phys.*, 2012, **14**, 11633–11638.

67 Y. Fu, S. Su, N. Zhang, Y. Wang, X. Guo and J. Xue, Dehydration-Determined Ion Selectivity of Graphene Subnanopores, *ACS Appl. Mater. Interfaces*, 2020, **12**, 24281–24288.

68 Z. Chen, C. Hu, C. Lu, J. Sun, Y. Zhang, F. Wang and J. Qu, Steric hindrance-induced dehydration promotes cation selectivity in trans-subnanochannel transport, *ACS Nano*, 2023, **17**(13), 12629–12640.

69 C. Lu, C. Hu, C. L. Ritt, X. Hua, J. Sun, H. Xia, Y. Liu, D. W. Li, B. Ma, M. Elimelech and J. Qu, In Situ Characterization of Dehydration during Ion Transport in Polymeric Nanochannels, *J. Am. Chem. Soc.*, 2021, **143**, 14242–14252.

70 C. L. Ritt, J. R. Werber, M. Wang, Z. Yang, Y. Zhao, H. J. Kulik and M. Elimelech, Ionization behavior of nanoporous polyamide membranes, *Proc. Natl. Acad. Sci. U. S. A.*, 2020, **117**, 30191–30200.

71 J. J. Velasco-Velez, C. H. Wu, T. A. Pascal, L. F. Wan, J. Guo, D. Prendergast and M. Salmeron, Interfacial water. The structure of interfacial water on gold electrodes studied by x-ray absorption spectroscopy, *Science*, 2014, **346**, 831–834.

72 J. N. Israelachvili and R. M. Pashley, Molecular layering of water at surfaces and origin of repulsive hydration forces, *Nature*, 1983, **306**, 249–250.

73 C. Y. Lee, J. A. McCammon and P. J. Rossky, The structure of liquid water at an extended hydrophobic surface, *J. Chem. Phys.*, 1984, **80**, 4448–4455.

74 G. Cicero, J. C. Grossman, E. Schwegler, F. Gygi and G. Galli, Water confined in nanotubes and between graphene sheets: a first principle study, *J. Am. Chem. Soc.*, 2008, **130**, 1871–1878.

75 L. Fumagalli, A. Esfandiar, R. Fabregas, S. Hu, P. Ares, A. Janardanan, Q. Yang, B. Radha, T. Taniguchi, K. Watanabe, G. Gomila, K. S. Novoselov and A. K. Geim, Anomalously low dielectric constant of confined water, *Science*, 2018, **360**, 1339–1342.

76 A. Razmjou, M. Asadnia, E. Hosseini, A. Habibnejad Korayem and V. Chen, Design principles of ion selective nanostructured membranes for the extraction of lithium ions, *Nat. Commun.*, 2019, **10**, 5793.

77 C. E. Ren, K. B. Hatzell, M. Alhabeb, Z. Ling, K. A. Mahmoud and Y. Gogotsi, Charge- and Size-Selective Ion Sieving Through Ti3C2Tx MXene Membranes, *J. Phys. Chem. Lett.*, 2015, **6**, 4026–4031.

78 R. Xu, Y. Kang, W. Zhang, B. Pan and X. Zhang, Two-dimensional MXene membranes with biomimetic sub-nanochannels for enhanced cation sieving, *Nat. Commun.*, 2023, **14**, 4907.

79 R. M. DuChanois, M. Heiranian, J. Yang, C. J. Porter, Q. Li, X. Zhang, R. Verduzco and M. Elimelech, Designing polymeric membranes with coordination chemistry for high-precision ion separations, *Sci. Adv.*, 2022, **8**, eabm9436.

80 C. Labbez, P. Fievet, A. Szymczyk, A. Vidonne, A. Foissy and J. Pagetti, Analysis of the salt retention of a titania membrane using the "DSPM" model: effect of pH, salt concentration and nature, *J. Membr. Sci.*, 2002, **208**, 315–329.

81 I. Shefer, O. Peer-Haim, O. Leifman and R. Epsztein, Enthalpic and Entropic Selectivity of Water and Small Ions in Polyamide Membranes, *Environ. Sci. Technol.*, 2021, **55**, 14863–14875.

82 F. Sheng, B. Wu, X. Li, T. Xu, M. A. Shehzad, X. Wang, L. Ge, H. Wang and T. Xu, Efficient Ion Sieving in Covalent Organic Framework Membranes with Sub-2-Nanometer Channels, *Adv. Mater.*, 2021, **33**, e2104404.

83 Y. Guo, Y. Ying, Y. Mao, X. Peng and B. Chen, Polystyrene Sulfonate Threaded through a Metal-Organic Framework Membrane for Fast and Selective Lithium-Ion Separation, *Angew. Chem., Int. Ed.*, 2016, **55**, 15120–15124.

84 C. Zhang, Y. Mu, W. Zhang, S. Zhao and Y. Wang, PVC-based hybrid membranes containing metal-organic frameworks for Li+/Mg2+ separation, *J. Membr. Sci.*, 2020, **596**, 117724.

85 H. Wang, Y. Zhai, Y. Li, Y. Cao, B. Shi, R. Li, Z. Zhu, H. Jiang, Z. Guo, M. Wang, L. Chen, Y. Liu, K. G. Zhou, F. Pan and Z. Jiang, Covalent organic framework membranes for efficient separation of monovalent cations, *Nat. Commun.*, 2022, **13**, 7123.

86 H. Zhang, X. Li, J. Hou, L. Jiang and H. Wang, Angstrom-scale ion channels towards single-ion selectivity, *Chem. Soc. Rev.*, 2022, **51**, 2224–2254.

87 H. Daiguji, Ion transport in nanofluidic channels, *Chem. Soc. Rev.*, 2010, **39**, 901–911.

88 R. Hatsuki, F. Yujiro and T. Yamamoto, Direct measurement of electric double layer in a nanochannel by electrical impedance spectroscopy, *Microfluid. Nanofluid.*, 2012, **14**, 983–988.

89 Y. Huang, X. Liu, S. Li and T. Yan, Development of mean-field electrical double layer theory, *Chin. Phys. B*, 2015, **25**(1), 016801.

90 J. Lu, H. Xu, H. Yu, X. Hu, J. Xia, Y. Zhu, F. Wang, H. A. Wu, L. Jiang and H. Wang, Ultrafast rectifying counter-directional transport of proton and metal ions in metal-

This journal is © The Royal Society of Chemistry 2024

Environ. Sci.: Water Res. Technol., 2024, **10**, 1305–1318 | **1317**

organic framework-based nanochannels, *Sci. Adv.*, 2022, **8**, eabl5070.

91 H. B. Park, J. Kamcev, L. M. Robeson, M. Elimelech and B. D. Freeman, Maximizing the right stuff: The trade-off between membrane permeability and selectivity, *Science*, 2017, **356**(6343), eaab0530.

92 H. F. Ridgway, J. Orbell and S. Gray, Molecular simulations of polyamide membrane materials used in desalination and water reuse applications: Recent developments and future prospects, *J. Membr. Sci.*, 2017, **524**, 436–448.

93 X. Sun, M. Di, J. Liu, L. Gao, X. Yan and G. He, Continuous Covalent Organic Frameworks Membranes: From Preparation Strategies to Applications, *Small*, 2023, e2303757, DOI: **10.1002/smll.202303757**.

94 Z. Lu, Y. Wei, J. Deng, L. Ding, Z. K. Li and H. Wang, Self-Crosslinked MXene (Ti3C2Tx) Membranes with Good Antiswelling Property for Monovalent Metal Ion Exclusion, *ACS Nano*, 2019, **13**, 10535–10544.

95 L. Chen, G. Shi, J. Shen, B. Peng, B. Zhang, Y. Wang, F. Bian, J. Wang, D. Li, Z. Qian, G. Xu, G. Liu, J. Zeng, L. Zhang, Y. Yang, G. Zhou, M. Wu, W. Jin, J. Li and H. Fang, Ion sieving in graphene oxide membranes via cationic control of interlayer spacing, *Nature*, 2017, **550**, 380–383.

1318 | *Environ. Sci.: Water Res. Technol.*, 2024, **10**, 1305–1318

This journal is © The Royal Society of Chemistry 2024